THE JOURNAL OF PHYSICAL CHEMISTRY A

Article

pubs.acs.org/JPCA

Thermochemistry of Alkali Metal Cation Interactions with Histidine: Influence of the Side Chain

P. B. Armentrout,*[,†] Murat Citir,[†,§] Yu Chen,[‡] and M. T. Rodgers*[,‡]

[†]Department of Chemistry, University of Utah, 315 South 1400 East, Room 2020, Salt Lake City, Utah 84112, United States

[‡]Department of Chemistry, Wayne State University, Detroit, Michigan 48202, United States

ABSTRACT: The interactions of alkali metal cations (M^+ = Na^+, K^+, Rb^+, Cs^+) with the amino acid histidine (His) are examined in detail. Experimentally, bond energies are determined using threshold collision-induced dissociation of the M^+(His) complexes with xenon in a guided ion beam tandem mass spectrometer. Analyses of the energy dependent cross sections provide 0 K bond energies of 2.31 ± 0.11, 1.70 ± 0.08, 1.42 ± 0.06, and 1.22 ± 0.06 eV for complexes of His with Na^+, K^+, Rb^+, and Cs^+, respectively. All bond dissociation energy (BDE) determinations include consideration of unimolecular decay rates, internal energy of reactant ions, and multiple ion-neutral collisions. These experimental results are compared to values obtained from quantum chemical calculations conducted previously at the MP2(full)/6-311+G(2d,2p), B3LYP/6-311+G(2d,2p), and B3P86/6-311+G(2d,2p) levels with geometries and zero point energies calculated at the B3LYP/6-311+G(d,p) level where Rb and Cs use the Hay−Wadt effective core potential and basis set augmented with additional polarization functions (HW*). Additional calculations using the def2-TZVPPD basis set with B3LYP geometries were conducted here at all three levels of theory. Either basis set yields similar results for Na^+(His) and K^+(His), which are in reasonable agreement with the experimental BDEs. For Rb^+(His) and Cs^+(His), the HW* basis set and ECP underestimate the experimental BDEs, whereas the def2-TZVPPD basis set yields results in good agreement. The effect of the imidazole side chain on the BDEs is examined by comparing the present results with previous thermochemistry for other amino acids. Both polarizability and the local dipole moment of the side chain are influential in the energetics.

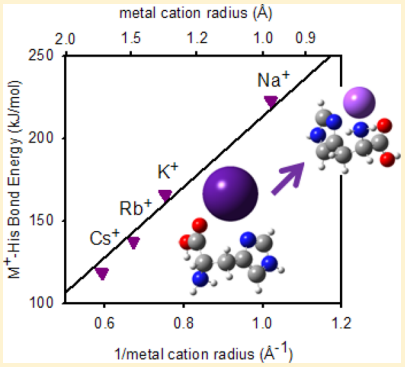

INTRODUCTION

A starting point for understanding how the biologically important alkali metal cations interact with proteins is to quantitatively assess their interactions with the simpler amino acids. Such intrinsic pairwise interactions, in the absence of complicating solvent effects, can form the basis of a "thermodynamic vocabulary"[1] of utility in enhancing our understanding of complicated biological systems. In the present study, we extend previous work on the absolute binding energies of alkali metal cations with amino acids[2−12] to examine Na^+, K^+, Rb^+, and Cs^+ binding with histidine (His), one of the basic amino acids. The importance of His interactions with metal ions in biological systems has been recognized for some time as His regulates the proper utilization of trace metals and is essential in their rapid excretion when present in excess.[13,14] His is often found at the catalytic sites of protein enzymes and is the precursor of the histamine hormone. The His molecule presents three potential coordination sites in aqueous solution. The imidazole nitrogen of histidine residues is a primary site for binding metal ions to proteins, although various crystal studies have shown that histidine can also use the carboxyl group and the amino nitrogen, depending on the pH.[15−20]

The pairwise interactions of alkali metal cations with the 20 common amino acids have been studied extensively both experimentally and theoretically.[2−12,21−28] Cooks' kinetic method[29,30] has been used to measure the relative cation binding affinities of most of the 20 common amino acids for both lithium[21,22,27] and sodium.[21,26] For sodium cation affinities, Bojesen et al.[21] found that the value for His was the second highest, lying only below that of arginine (Arg) in their relative measurements. This order was confirmed in the more quantitative study of Kish et al.,[26] where the sodium cation binding affinity for His was found to lie 51.7 kJ/mol above that of Ala, which anchors their absolute affinity scale at 167 ± 8 kJ/mol, such that D_{298}(Na^+−His) = 219 ± 8 kJ/mol. Histidine is not included among the experimental lithium cation binding affinities of Feng et al.[27] or potassium cation binding affinities compiled by Tsang and co-workers[31] but is found in the relative binding affinity determinations of Cu^+ and Ag^+,[32,33] where it again is one of the strongest binding amino acids. The only previous rubidium and cesium cation binding affinities (experimental or theoretical) to amino acids come from recent studies that include only Gly, Pro, Ser, Thr, and Cys.[10−12]

Theoretical studies of these alkali metal cation amino acid complexes[2−12,23,34−47] indicate that metal cations bind electrostatically to the functional groups of the amino acid backbone and side chain. Such theoretical predictions have been confirmed by thermodynamic studies involving threshold

Received: October 15, 2012
Revised: November 17, 2012
Published: November 19, 2012

collision-induced dissociation (TCID) studies of various metalated α-amino acids,[2−12] and by infrared multiple photon dissociation (IRMPD) action spectra of sodiated Gly and proline (Pro),[28] and metalated tryptophan (Trp),[39] arginine (Arg),[40] serine (Ser),[41] threonine (Thr),[42] aspartic and glutamic acid (Asp, Glu),[43] asparagine (Asn),[45] methionine (Met),[46] and cysteine (Cys).[47] Recently, we extended this IRMPD and theoretical work to the gas-phase structures of His cationized with Li^+, Na^+, K^+, Rb^+, and Cs^+.[48] To identify the structures present in that experimental study, the IRMPD spectra were compared to single photon spectra calculated at B3LYP/6-311+G(d,p) (Li^+, Na^+, and K^+ complexes) and B3LYP/HW*/6-311+G(d,p) (Rb^+ and Cs^+ complexes) levels of theory, where HW* indicates that the Hay−Wadt effective core potential[49] with additional polarization functions was used for Rb and Cs.[50] Single point energy calculations were carried out at the B3LYP, B3P86, and MP2(full) levels using the HW*/6-311+G(2d,2p) basis set. On the basis of these experiments and calculations, Li^+(His) and Na^+(His) complexes were found to have charge-solvated, tridentate structures where the metal cation binds to the carbonyl oxygen, backbone amino nitrogen, and nitrogen atom of the imidazole side chain, [CO,N_α,N_π], in agreement with the predicted ground state conformers of these complexes. The larger alkali metal cation complexes, K^+(His), Rb^+(His), and Cs^+(His), have similar IRMPD spectra that are considerably more complex than those of Li^+(His) and Na^+(His). For these larger complexes, the bidentate [CO,N_π] conformers, where the metal cation binds to the carbonyl oxygen and nitrogen atom of the imidazole side chain, are dominant contributors, along with contributions from the tridentate [CO,N_α,N_π] and bidentate [COOH] conformers. These three conformers are the lowest energy conformers found computationally for all of the alkali metal cations.

To further characterize metal cation binding to His, the present study measures the binding affinities of Na^+, K^+, Rb^+, and Cs^+ with His using TCID methods in a guided ion beam tandem mass spectrometer (GIBMS). These results are then compared to theoretical predictions as well as previous thermochemistry for alkali metal cation complexes with other amino acids. These comparisons allow an examination of how binding energies of the alkali metal cation histidine complexes vary with conformation and elucidate how variations in the side chain influence the strength of alkali metal cation binding.

EXPERIMENTAL AND COMPUTATIONAL SECTION

General Experimental Procedures. The TCID experiments were conducted on two GIBMS instruments located at the University of Utah for the sodium and potassium complexes and Wayne State University for the rubidium and cesium complexes. Both instruments have been described in detail previously.[51−53] Briefly, M^+(His) complexes are formed in electrospray ionization (ESI) sources[54] under conditions similar to those described previously.[55] The ESI is operated using a 50:50 by volume H_2O/MeOH solution with ~10^{-4} M amino acid and alkali metal chloride salt (all chemicals purchased from Sigma-Aldrich), which is syringe-pumped at a rate of 0.04 mL/h into a 35 gauge stainless steel needle biased at ~2000 V. Addition of proline to the solution was used to stabilize the electrospray conditions. Ionization occurs over the ~5 mm distance from the tip of the needle to the entrance of the capillary, biased at ~35 V. Ions are directed by a capillary heated to 80 °C into vacuum and a radio frequency (rf) ion funnel,[56] wherein they are focused into a tight beam. Ions exit the ion funnel and enter an rf hexapole ion guide that traps them radially. Here the ions undergo multiple collisions (>10^4) with the ambient gas (largely solvent) and become thermalized to room temperature.[7,57−60]

The ions are then mass analyzed using a magnetic momentum analyzer, injected into a radio frequency (rf) octopole ion beam guide,[61] where ions are radially trapped and their kinetic energy controlled. The octopole passes through a gas cell that contains Xe at pressures of approximately 0.05, 0.10, and 0.20 mTorr. To obtain data under rigorously single collision conditions, reaction cross sections are extrapolated to zero reactant pressure prior to threshold analysis.[62] A complete set of pressure measurements was reproduced at least two times for each system. All product and residual reactant ions drift to the end of the octopole where they are extracted, mass analyzed using a quadrupole mass filter, and detected by a high voltage conversion dynode-secondary electron scintillation detector[63] interfaced with fast pulse counting electronics. The raw ion intensities are converted to cross sections as described elsewhere.[51] The absolute cross sections are estimated to be accurate to ±20% with relative uncertainties of ±5%. Laboratory (lab) collision energies are converted to center-of-mass (CM) energies using the equation $E_{CM} = E_{lab}\, M/(M + m)$, where M and m are the reactant neutral and ion masses, respectively. All energies cited below are in the CM frame unless otherwise noted. The absolute energy scale and the corresponding full width at half-maximum (fwhm) of the ion beam kinetic energy distribution are determined by using the octopole as a retarding energy analyzer.[51] The energy spread is nearly Gaussian and has a typical fwhm in the lab frame of 0.1−0.2 eV for Na^+(His) and K^+(His) systems and 0.4−0.5 eV for Rb^+(His) and Cs^+(His) systems.

Threshold Analysis. Analysis of the data to extract threshold energies is achieved by fitting the energy dependent cross sections in the threshold region using eq 1,

$$\sigma_j(E) = (N\sigma_0/E) \sum g_i \int_{E_0-E_i}^{E} [1 - e^{-k(E^*)\tau}] (E - \varepsilon)^{n-1} d(\varepsilon) \quad (1)$$

where σ_0 is an adjustable energy-independent scaling parameter, n is an adjustable parameter that describes the energy deposition efficiency during collision,[52] E is the relative kinetic energy of the reactants, and E_0 represents the CID threshold energy at 0 K. E_i are the internal energies of the rovibrational states i of the reactant ion with populations g_i, where $\Sigma g_i = 1$, such that $E + E_i$ is the total energy available to the colliding reactants. Vibrational frequencies and rotational constants used to calculate E_i and g_i are obtained from the calculations outlined in the next section. The Beyer−Swinehart−Stein−Rabinovitch algorithm[64−66] is used to evaluate the density of the rovibrational states and the relative populations g_i are calculated for a Maxwell−Boltzmann distribution at 300 K. Equation 1 also includes the effects of unimolecular dissociation kinetics during the time available for dissociation, $\tau \sim 5 \times 10^{-4}$ s at Utah[52] and ~1×10^{-4} s at WSU.[53] The kinetics are estimated using Rice−Ramsperger−Kassel−Marcus (RRKM) theory,[67−69] as described in detail elsewhere,[70−72] where ε is the energy transferred from translation into internal energy of the complex during the collision, and E^* is the internal energy of the energized molecule (EM), i.e., $E^* = \varepsilon + E_i$. The term $k(E^*)$ is the

unimolecular rate constant for dissociation of the EM, as defined by RRKM theory in eq 2,

$$k(E^*) = dN_{vr}^{\dagger}(E^*-E_0)/hr_{vr}(E^*) \quad (2)$$

where d is the reaction degeneracy, h is Planck's constant, $N_{vr}^{\dagger}(E^*-E_0)$ is the sum of rovibrational states of the transition state (TS) at an energy $E^* - E_0$, and $\rho_{vr}(E^*)$ is the density of rovibrational states of the EM at the available energy, E^*. To evaluate the rate constant in eq 2, vibrational frequencies and rotational constants for the EM and TS are required. Because the metal−ligand interactions in the complexes studied here are mainly long-range electrostatic interactions (ion-dipole, ion-quadrupole, and ion-induced dipole), the most appropriate model for the TS for M^+(His) complexes dissociating to M^+ + His is a loose association of the ion and neutral ligand,[2,3,73−76] even for multidentate ligands.[58,77−80] Therefore, the TSs are treated as product-like, such that the TS frequencies are those of the dissociated products. The transitional frequencies are treated as rotors, a treatment that corresponds to a phase space limit (PSL), as described in detail elsewhere.[70,71] The three transitional mode rotors have rotational constants equal to those of the ligand product. The two-dimensional external rotations are treated adiabatically but with centrifugal effects included.[81] In the present work, the adiabatic two-dimensional rotational energy is treated using a statistical distribution with an explicit summation over all possible values of the rotational quantum number.[70]

When compared to the experimental data, the cross section calculated using eq 1 is convoluted over the kinetic energy distribution of the ion beam and thermal energy distribution of the neutral collision gas (Doppler broadening), as described elsewhere.[51] Uncertainties in the fitting parameters are obtained from variations associated with different data sets, the parameter N, changes in the vibrational frequencies (±10%), variations in τ by a factor of 2, and the uncertainty in the absolute energy scale, ±0.05 eV (lab).

In deriving the final optimized bond energies at 0 K, two assumptions are made. First, there is no activation barrier in excess of the endothermicity for the loss of ligands, which is generally true for ion−molecule reactions, especially the heterolytic noncovalent bond cleavages considered here.[82] Second, the measured threshold is assumed to correspond to dissociation of the lowest energy conformer of the reactant to the metal cation and neutral ligand product in its lowest energy conformation. Given the relatively long experimental time frame available for the energized complexes to explore phase space, we assume that the dissociating products are able to rearrange to their ground state conformations upon dissociation. The appropriateness of this assumption for the His ligand is nicely verified by the good agreement between our experimental results with theoretical values, as discussed below.

Computational Details. Previous geometry optimizations of the M^+(His) complexes[48] were conducted at the B3LYP/6-311+G(d,p) level of theory using Gaussian 09.[83] Zero point energies determined at this level were scaled by 0.989.[84] Single point energy calculations were conducted using these geometries with the 6-311+G(2d,2p) basis set at the B3LYP, B3P86, and MP2(full) levels of theory. For complexes of the heavier metal cations, Rb^+ and Cs^+, calculations utilized the effective core potentials (ECPs) and valence basis sets of Hay and Wadt[49] with a single d polarization function (exponents of 0.24 and 0.19, respectively) added,[50] which we call HW*. To augment these results, we have redetermined the geometries of the lowest energy conformers using B3LYP with the def2-TZVPPD basis set, which is of triple-ζ valence quality plus double polarization and diffuse functions for all elements.[85] This basis set uses small core ECPs developed by Leininger et al. for Rb and Cs.[86] Recent studies have demonstrated that the def2 basis sets provide more accurate thermochemistry for Rb^+ and Cs^+ complexes than the HW* basis set.[11,12,80]

Basis set superposition errors (BSSE) in all bond dissociation energy calculations were estimated using the full counterpoise (cp) method.[87,88] Previous work[2,3,76,89,90] has indicated that BSSE corrections on alkali metal systems are generally small for DFT calculations and we find this to be true here as well. Both B3LYP and B3P86 calculations have BSSE corrections of 0.4−4 kJ/mol when the HW*/6-311+G(2d,2p) basis set is used, but only 0−2 kJ/mol for the def2-TZVPPD basis set. MP2(full) values have larger BSSE corrections of 5−15 kJ/mol when the HW*/6-311+G(2d,2p) basis set is used and 9−22 kJ/mol for def2-TZVPPD.

RESULTS

Theory: Histidine. The conformations of histidine have been explored theoretically before, both for the canonical tautomer, in which a hydrogen atom is bonded to N_τ of the imidazole side chain, His[N_τH],[91] and for the tautomer in which the hydrogen has moved to N_π, His[N_πH].[92] Here, the atoms of His are named according to the IUPAC Compendium of Chemical Terminology ("Gold Book"),[93] in which positions of the nitrogen atoms of the imidazole ring relative to the side chain are denoted by *pros* ("near", abbreviated π and also referred to as N_1) and *tele* ("far", abbreviated τ or N_3). We distinguish conformers by a description of the histidine orientation, named by a series of dihedral angles starting from the carboxylic acid hydrogen of the backbone and going to the imidazole side-chain nitrogen (N_π) (∠HOCC, ∠OCCC, ∠CCCC, and ∠CCCN$_\pi$, respectively). Dihedral angles are distinguished as cis (c, for angles between 0−45°), gauche (g, 45−135°), or trans (t, 135−180°), and + or −, indicating their sign when necessary to distinguish similar structures. Forty-two and forty conformers, respectively, were located in the previous studies and covered a range of 60 kJ/mol in relative energy. The lowest of these for each tautomer, His[N_τH]ctgg and His[N_πH]ctgg, are shown in Figure 1 along with the His[N_τH]cgtg conformer next highest in energy, as reoptimized at the B3LYP/6-311+G(d,p) level of theory used here. In all cases, the structure is stabilized by an OH···NH_2 hydrogen bond, which is indicated by the proximity of the H atom to the

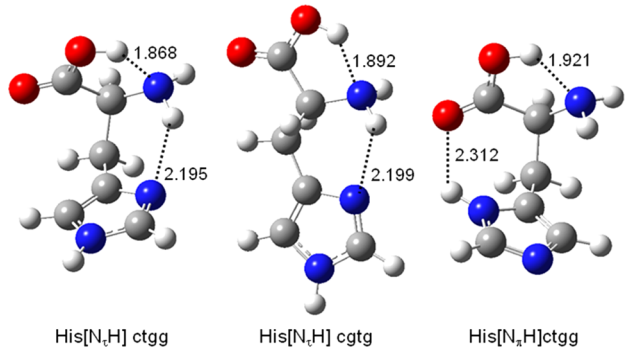

Figure 1. Low energy structures of His calculated at the B3LYP/6-311+G(d,p) level. Dashes indicate hydrogen bonds with lengths shown in Å.

dx.doi.org/10.1021/jp310179c | J. Phys. Chem. A 2012, 116, 11823−11832

nitrogen heteroatom and by elongation of the OH bond (by 0.015−0.019 Å, with the longest extension correlating with the shortest hydrogen bond). The His[N_τH] structures also have a NH···N_π hydrogen bond (here the NH covalent bond elongates by ∼0.007 Å), which is replaced by a N_πH···OC hydrogen bond in the His[N_πH] tautomer (N_πH elongation of 0.004 Å). Relative single point energies of these two conformers are calculated at B3LYP, B3P86, and MP2(full) levels of theory using the HW*/6-311+G(2d,2p) basis set and including zero point energy (ZPE) corrections. These results all find that His[N_τH]ctgg is lower in energy by 2.6−3.1 kJ/mol, consistent with the shorter hydrogen bonds for this tautomeric form, Figure 1. Likewise the lowest excited conformer, His[N_τH]cgtg, is found to lie 2.4−6.1 kJ/mol above the ground state conformer, His[N_τH]ctgg, in good agreement with Huang et al. who calculated excitation energies of 2.7−7.2 kJ/mol.[91] Notably, several previous works examining metal cation complexes of His have utilized the higher energy His[N_πH] tautomer as the ground state conformation in dissociation studies.[94,95]

Theory: M^+(His). A full exploration of the conformations of M^+(His) complexes for all five alkali metal cations was conducted in conjunction with our IRMPD study of these species (where the N_1 and N_3 nomenclature was used for the nitrogens of the imidazole side chain rather than N_π and N_τ, respectively, used here).[48] This enabled identification of the likely conformers formed by electrospray ionization. Only three conformers, shown in Figure 2, are needed for this purpose.

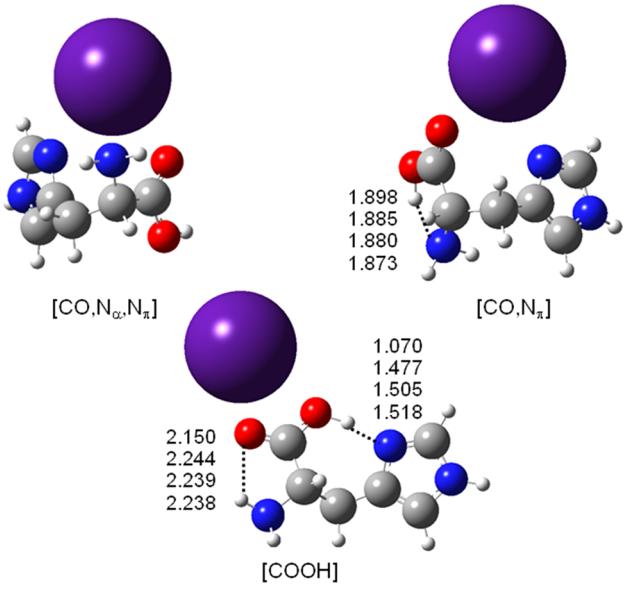

Figure 2. Cs^+(His) low energy structures calculated at the B3LYP/def2-TZVPPD level. Dashes indicate hydrogen bonds with lengths shown in Å for Na^+(His) (top), K^+(His), Rb^+(His), and Cs^+(His) (bottom). Note that the large changes in hydrogen bond lengths for Na^+(His) [COOH] are because this structure converts to the zwitterionic analogue.

These all involve metal cation binding to His[N_τH], with M^+(His[N_πH]) conformers lying much higher in energy. Table 1 lists the relative energies of these three conformers at 0 K calculated previously along with additional values obtained here using the def2-TZVPPD basis set. To identify these conformers, we use the nomenclature established previously for M^+(Gly),[2,3,96,97] where the notation in brackets describes the metal binding sites for each conformer, followed by the description of the histidine orientation detailed above.

At all levels of theory, the structure for the ground state conformer (GSC) of Li^+(His) and Na^+(His) is the [CO,N_α,N_π]-tgcg conformer, a tridentate structure in which the metal cation binds to the carbonyl oxygen, backbone amino nitrogen (N_α), and the N_π side-chain nitrogen. For these smaller alkali metal cation complexes, the alternative structures found to be low-lying for the larger metal cations are >8 kJ/mol higher in energy, Table 1. These calculations are consistent with the IRMPD spectra that find evidence for only the [CO,N_α,N_π] conformer.[48] For Rb^+(His) and Cs^+(His), the GSC is either [CO,N_π]-ctg$_-$g$_+$ or [COOH]-cgg$_+$g$_-$. The DFT calculations indicate that these two bidentate structures are nearly isoenergetic, lying within 3 kJ/mol of one another, whereas MP2 calculations find the [COOH] structure is higher by 7−13 kJ/mol. For these heavier complexes, the tridentate [CO,N_α,N_π] conformer is now 7−20 kJ/mol above the GSC at the DFT level but only 2−11 kJ/mol higher for MP2 calculations. The K^+(His) complex is clearly intermediate in behavior, with DFT favoring the [CO,N_π] conformer as the GSC by 1−5 kJ/mol and MP2 indicating that [CO,N_α,N_π] is lower by 2−3 kJ/mol. The IRMPD spectra of K^+(His), Rb^+(His), and Cs^+(His) are all similar with evidence for all three of these conformations. For Cs^+(His), features associated with [CO,N_α,N_π] are diminished compared to the lighter complexes, consistent with the relative energetics at all levels of theory.

Cross Sections for Collision-Induced Dissociation. Experimental cross sections were obtained for the interaction of Xe with four M^+(His) complexes, where M^+ = Na^+, K^+, Rb^+, and Cs^+, as a function of collision energy. Figure 3 shows representative data extrapolated to zero pressure of Xe for collision-induced dissociation (CID) of all four complexes. Over the energy ranges examined, the loss of the intact amino acid, reaction 3, is seen in all four M^+(His) systems, and this is the only dissociation channel observed.

$$M^+(\text{His}) + \text{Xe} \rightarrow M^+ + \text{His} + \text{Xe} \quad (3)$$

(In the Na^+(His) system, a product corresponding to loss of 31 ± 1 m/z was also observed with a cross section that varied over time and an apparent threshold near 0.5 eV. This behavior is consistent with loss of an intact methanol molecule from a contaminant in the beam. Because the magnitudes of the Na^+ cross section did not vary with time, the presence of this contaminant does not affect the results shown in Figure 3a.) The relative thresholds of the cross sections for process 3 decrease from Na^+ to K^+ to Rb^+ to Cs^+, reflecting the decrease in the binding energy to the intact amino acid. This is consistent with previous threshold CID bond dissociation energy measurements of metal cationized amino acids[2−12] and many other ligands.[98]

The Li^+(His) system was also examined but reaction 3 was very weak, sufficiently so that no thermochemical information could be obtained. The dominant processes observed in this system were loss of NH_3, loss of CO + H_2O, and formation of NH_4^+.

Threshold Analysis and Results. Histidine losses in reactions 3 were modeled using eq 1. Figure 3 shows that the experimental cross sections are reproduced well by eq 1 over extended energy and magnitude ranges. The optimized parameters of eq 1 for all systems using molecular parameters for the ground state conformers and PSL transition states

Table 1. B3LYP, B3P86, and MP2(full) 0 K Relative Energies (kJ/mol) of Low-lying Conformers of M^+(His)[a]

structure	dihedrals[b]	Li^+(His)	Na^+(His)	K^+(His)	Rb^+(His)	Cs^+(His)
[CO,$N_\omega N_\pi$]	tgcg	**0.0**, **0.0**, **0.0**	**0.0**, **0.0**, **0.0**	0.8, 3.8, **0.0**	8.4, 12.3, 3.8	15.8, 19.6, 11.4
			0.0, ***0.0***, ***0.0***	*1.9*, *5.2*, ***0.0***	*6.9*, *9.9*, *1.7*	*10.9*, *14.5*, *5.8*
[CO,N_π]	ctg$_-$g$_+$	21.1, 20.4, 33.9	12.8, 9.2, 16.6	**0.0**, **0.0**, 3.0	**0.0**, 0.9, **0.0**	2.0, 2.8, **0.0**
			11.8, *8.0*, *15.9*	***0.0***, ***0.0***, *1.9*	***0.0***, ***0.0***, ***0.0***	*0.6*, *1.6*, ***0.0***
[COOH]	cgg$_+$g$_-$	46.1, 42.3, 54.7[c]	23.3, 18.8, 34.4[c]	4.6, 2.1, 12.5	0.7, **0.0**, 7.0	**0.0**, **0.0**, 7.8
			22.8, *18.5*, *37.1*[c]	*5.1*, *2.8*, *15.1*	*2.0*, *0.3*, *13.4*	***0.0***, ***0.0***, *10.8*

[a]B3LYP, B3P86, and MP2(full) values calculated using the 6-311+G(2d,2p) basis sets with structures and zero point energies calculated at the B3LYP/6-311+G(d,p) level of theory. Values for Rb and Cs use the HW* basis set on the metal. Italics indicate values calculated using the def2-TZVPPD basis set with structures and zero point energies calculated at the B3LYP/def2-TZVPPD level of theory. Bold indicates the ground state conformer. [b]Dihedral angles for ∠HOCC, ∠OCCC, ∠CCCC, and ∠CCCN$_\pi$. [c]Collapses to the zwitterionic form, [CO_2^-]-cgg$_+$g$_-$, having the specified energies.

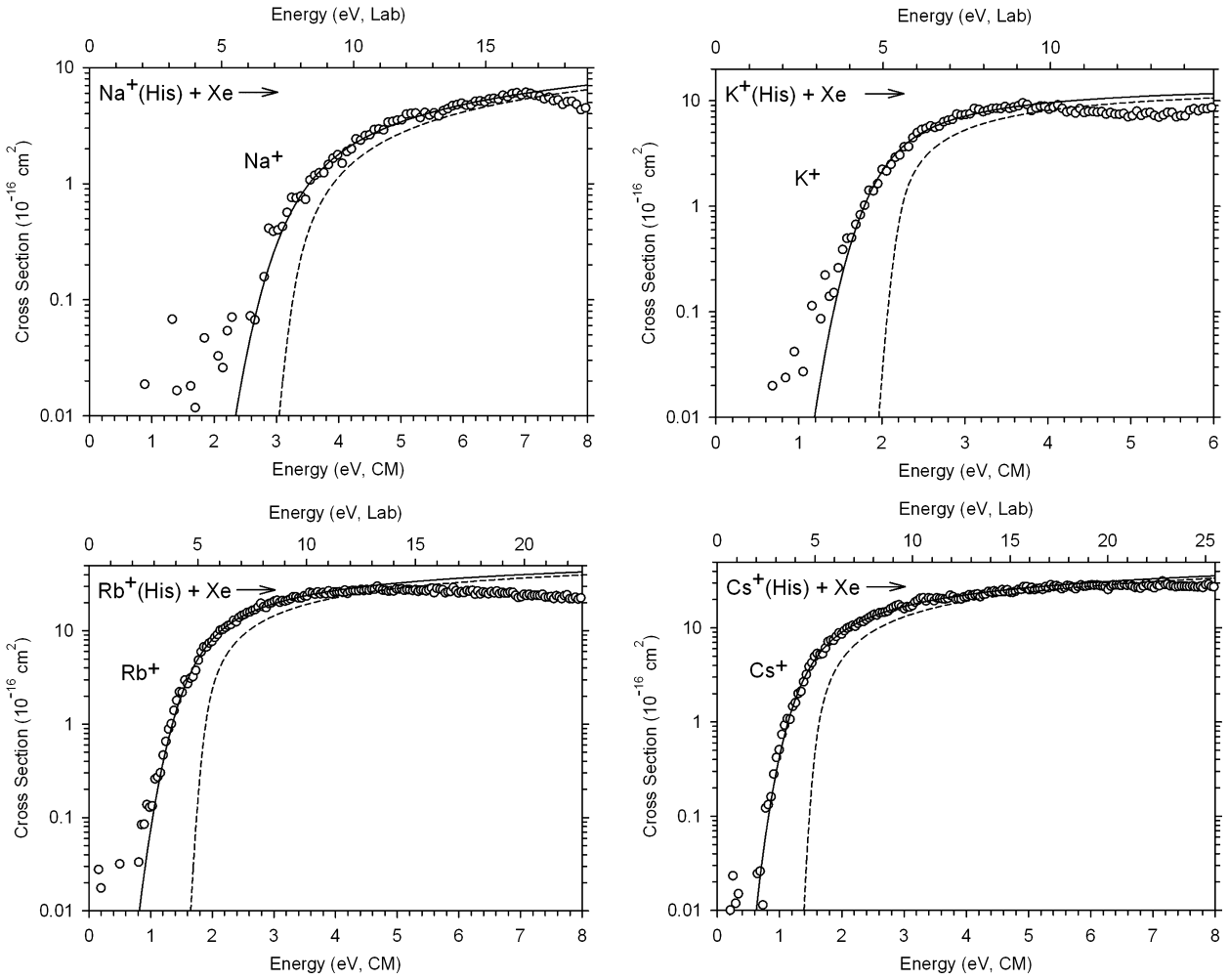

Figure 3. Zero pressure extrapolated cross sections for collision-induced dissociation of Na^+(His), K^+(His), Rb^+(His), and Cs^+(His) with Xe as a function of kinetic energy in the center-of-mass frame (lower *x*-axis) and the laboratory frame (upper *x*-axis). Solid lines show the best fit to the data using the model of eq 1 convoluted over the neutral and ion kinetic and internal energy distributions. Dashed lines show the model cross sections in the absence of experimental kinetic broadening for reactants with an internal energy of 0 K.

calculated at the B3LYP/6-311+G(d) level are reported in Table 2. As discussed below, different levels of theory predict different ground state conformers of some of the M^+(His) complexes; hence the data are analyzed independently with each possible ground state conformer. It was also checked whether using a different His[N_τH] conformation as the product influenced the results but thresholds remained the same within 0.01 eV. Use of the alternative tautomer, His[N_πH], reduces the thresholds by 0.02−0.03 eV; however, this tautomer is unlikely to be formed from the ground state conformers of the M^+(His) complexes, for reasons discussed previously in related systems.[99] The difference between threshold values with and without RRKM lifetime analysis in Table 2 equals the kinetic shift for M^+(His): 0.84, 0.44, 0.35, and 0.28 eV for Na^+, K^+, Rb^+, and Cs^+, respectively, consistent with the usual trend of increasing kinetic shift with increasing E_0. These shifts are substantially higher than for the analogous alkali metal cation complexes of many other amino acids where

dx.doi.org/10.1021/jp310179c | J. Phys. Chem. A 2012, 116, 11823−11832

Table 2. Fitting Parameters of Eq 1, Threshold Dissociation Energies at 0 K, and Entropies of Activation at 1000 K for CID of M^+(His) with Xe[a]

reactant	conformer	products	σ_0	n	E_0 (eV)[b]	E_0(PSL) (eV)	$\Delta S^{\ddagger}_{1000}$ [J/(mol K)]
Na^+(His)	[CO,N_ω,N_π]	Na^+ + His	6.2 (1.5)	1.4 (0.1)	3.14 (0.11)	2.31 (0.11)	49 (2)
K^+(His)	[CO,N_ω,N_π]	K^+ + His	18.5 (2.4)	1.0 (0.1)	2.14 (0.08)	1.70 (0.08)	41 (2)
	[CO,N_π]	K^+ + His	18.6 (2.4)	1.0 (0.1)		1.69 (0.08)	42 (2)
Rb^+(His)	[CO,N_π]	Rb^+ + His	38.0 (3.2)	1.2 (0.1)	1.78 (0.06)	1.42 (0.06)	34 (2)
	[COOH]	Rb^+ + His	38.4 (3.2)	1.2 (0.1)		1.43 (0.06)	30 (2)
Cs^+(His)	[CO,N_π]	Cs^+ + His	24.5 (1.0)	1.3 (0.1)	1.50 (0.05)	1.21 (0.05)	20 (2)
	[COOH]	Cs^+ + His	24.3 (1.0)	1.3 (0.1)		1.24 (0.05)	26 (2)

[a]Uncertainties are listed in parentheses. [b]Does not include lifetime effects.

Table 3. Enthalpies and Free Energies of M^+(His) Binding at 0 and 298 K in kJ/mol[a]

complex	conformer	ΔH_0[b]	$\Delta H_{298} - \Delta H_0$[c]	ΔH_{298}	$T\Delta S_{298}$[c]	ΔG_{298}
Na^+(His)	[CO,N_ω,N_π]	222.5 (11.0)	1.8 (0.3)	224.3 (11.0)	35.5 (3.7)	188.8 (11.6)
K^+(His)	[CO,N_ω,N_π]	163.9 (8.0)	0.6 (0.4)	164.5 (8.0)	32.6 (3.6)	131.9 (8.8)
	[CO,N_π]	163.1 (8.0)	0.9 (0.4)	164.0 (8.0)	32.2 (3.7)	131.8 (8.8)
Rb^+(His)	[CO,N_π]	137.3 (5.6)	0.4 (0.5)	137.7 (5.6)	30.6 (3.7)	107.0 (6.7)
	[COOH]	137.6 (5.6)	0.7 (0.5)	138.2 (5.6)	30.8 (3.7)	107.4 (6.7)
Cs^+(His)	[CO,N_π]	117.0 (5.2)	−0.1 (0.5)	116.9 (5.2)	26.6 (3.6)	90.3 (6.4)
	[COOH]	119.5 (5.2)	0.2 (0.5)	119.8 (5.2)	29.4 (3.7)	90.4 (6.4)

[a]Uncertainties in parentheses. [b]Experimental values from this work (Table 2). [c]Values were computed using standard formulas and molecular constants calculated at the B3LYP/6-311+G(d,p) level. Uncertainties correspond to 10% variations in the vibrational frequencies of the ligands and 2-fold variations in the metal ligand-frequencies.

Table 4. Experimental and Theoretical Binding Energies (kJ/mol) at 0 K for M^+(His)

		experiment		theory[a]			
complex	conformer	this work[b]	literature[c]	B3LYP (cp)	B3P86 (cp)	MP2 (full, cp)	MP2(full)
Na^+(His)	[CO,N_ω,N_π]	222.5 (11.0)	217 (8)	230.2, *232.6*	220.0, *222.6*	215.7, *220.6*	229.3, *235.4*
K^+(His)	[CO,N_ω,N_π]	163.9 (8.0)		156.8, *154.7*	153.4, *150.8*	**156.2**, *154.8*	**163.8**, ***169.5***
	[CO,N_π]	163.1 (8.0)		**157.9**, ***157.0***	**157.5**, ***156.3***	154.4, ***155.2***	160.8, *167.7*
Rb^+(His)	[CO,N_π]	137.3 (5.6)		**127.6**, ***137.3***	128.1, ***138.1***	**125.8**, ***140.0***	**138.4**, ***158.5***
	[COOH]	137.6 (5.6)		127.3, *135.7*	**129.4**, ***138.1***	121.8, *131.5*	131.3, *145.1*
Cs^+(His)	[CO,N_π]	117.0 (5.2)		108.6, *123.4*	110.4, *126.2*	**112.0**, ***130.7***	**124.2**, ***142.6***
	[COOH]	119.5 (5.2)		**111.0**, ***124.0***	**113.6**, ***127.9***	107.2, *122.5*	116.4, *131.8*
MAD[d]				7.8 (1.9)	5.6 (2.3)	7.5 (2.9)	3.8 (3.7)
				5.2 (4.2)	*3.9 (4.2)*	*6.5 (5.4)*	*16.4 (9.0)*

[a]Geometry optimizations and zero point energy corrections calculated at the B3LYP/6-311+G(d,p) level. Final energies are taken from single point energies calculated at the levels indicated using 6-311+G(2d,2p) basis sets including counterpoise (cp) corrections, except as noted. Values in italics calculated using the def2-TZVPPD basis set. [b]Values from Table 2. Uncertainties in parentheses. [c]Corrected from 298 K value of Kish et al.,[26] anchored to Ala (222 ± 8 kJ/mol if anchored to our Gly value, see text). [d]Mean absolute deviations of predicted ground state conformers (in bold) from experiment. Uncertainties in parentheses.

the side-chains are all smaller,[2,3,5−12] but are very similar to those for sodium and potassium cation complexes of phenylalanine (Phe), which has a side chain of similar size to His, and smaller than the analogous complexes of tyrosine (Tyr) and tryptophan (Trp), with more complicated side chains.[4] Thus, the size of the kinetic shift increases with the size of the ligand and the resultant increase in vibrational frequencies. The relatively large kinetic shifts found here indicate the importance of incorporating RRKM theory into the threshold analysis when dealing with such complex systems.

Table 2 also includes $\Delta S^{\ddagger}_{1000}$ values when the ground state His[N_τH]ctgg conformer is the product, which range from 20 to 50 J/(mol K). These values indicate loose transition states for the M^+(His) systems, consistent with the analysis assumed and the range of values outlined by Lifshitz.[100] Use of alternative conformations of the His product lead to changes in these entropies of activation, e.g., His[N_τH]cgtg lowers the $\Delta S^{\ddagger}_{1000}$ values by 3−7 J/(mol K).

Conversion from 0 to 298 K and Excited Conformers. Conversion from 0 K bond energies to 298 K bond enthalpies and free energies is accomplished using the rigid rotor/harmonic oscillator approximation with rotational constants and vibrational frequencies calculated at the B3LYP/6-311+G(d,p) level. These ΔH_{298} and ΔG_{298} values along with the conversion factors and 0 K enthalpies measured here are reported in Table 3. The uncertainties listed are determined by scaling most of the vibrational frequencies by ±10% along with 2-fold variations in the metal−ligand frequencies.

We also calculated the relative ΔG_{298} values for the three lowest energy structures of each M^+(His) complex. In general, the relative ΔG_{298} excitation energies are comparable to the analogous differences in the ΔH_0 values (Table 1) although the free energies of the [CO,N_ω,N_π] conformers increase by several kJ/mol relative to the other conformers because the tridentate binding restricts the flexibility of the complex more. Using the ΔG_{298} values to calculate an equilibrium population of

dx.doi.org/10.1021/jp310179c | J. Phys. Chem. A 2012, 116, 11823−11832

conformers shows that the calculated ground state structures for each M^+(His) system should be dominant in the room temperature ion sources. Excited conformers are calculated to comprise less than 5% of the total for Na^+(His) with the [CO,N_α,N_π]-tgcg conformer being the only significant contributor. For K^+(His), the [CO,N_π] conformer comprises 29−68% of the calculated population, with the [COOH] conformer contributing 0−28%, and [CO,N_α,N_π] adding 6−70%. For Rb^+(His), these percentages change to 32−81%, 0−61%, and 0−29%, respectively, whereas they are 46−98%, 0−54%, and 0−3%, respectively, for Cs^+(His).

As noted above, the effect of having a different conformer populating the K^+(His), Rb^+(His), and Cs^+(His) complexes generated in the ion sources was examined by analyzing the data using the molecular parameters of each of the possible ground state conformers. In all cases, the threshold energies change by less than 3 kJ/mol, within experimental uncertainties. Thus, even if a distribution of conformers were present, it would not affect the final thermochemical values. Our best experimental bond dissociation energies (BDEs) are taken as averages of the results for each conformation, with uncertainties that reflect the ambiguity of the ground state conformer assignment.

DISCUSSION

Comparison of Theoretical and Experimental Bond Dissociation Energies. The experimental threshold energies presented in Table 2 are equivalent to the M^+−His BDEs at 0 K. The theoretical BDEs for the M^+(His) complexes, where M^+ = Na^+, K^+, Rb^+, and Cs^+ calculated at three levels of theory with two basis sets for all metal cations are compared to the experimental values in Table 4. We find that all three theoretical methods (B3LYP, B3P86, and MP2) yield BDE values for M^+(His) that are fairly similar but can differ for a single system by 7−20 kJ/mol. Mean absolute deviations (MADs) between experiment and the various levels of theory examined range from 4 to 16 kJ/mol (Table 4). Overall, all three levels of theory give comparable agreement with the experimental values, except for the MP2(full)/def2-TZVPPD with no counterpoise corrections. Note that not including kinetic shift effects in the data analysis would shift the experimental values such that they would no longer agree with theory within experimental uncertainties for all metal cations, clearly illustrating the importance of including the unimolecular decay rates in the threshold analyses.

The def2-TZVPPD basis set performs slightly better than the HW*/6-311+G(2d,2p) basis set, primarily because values for Rb^+(His) and Cs^+(His) obtained using the def2-TZVPPD basis set are systematically higher than values obtained using HW*/6-311+G(2d,2p), by an average of 12.7 ± 3.3 kJ/mol. For Na^+(His) and K^+(His), the two basis sets give comparable results, which demonstrates that the primary distinction between the basis sets is the more complete description of Rb and Cs by def2-TZVPPD. Using the ground state conformers of Rb^+(His) and Cs^+(His) in all cases, the HW*/6-311+G(2d,2p) values are systematically low and have a MAD from the experimental values of 8.1 ± 2.4 kJ/mol (7.1 ± 3.2 kJ/mol if the MP2(full,nocp) values are included), whereas the def2-TZVPPD values have a MAD of 5.0 ± 5.3 kJ/mol (9.6 ± 9.7 kJ/mol including the MP2(full,nocp) value). There is little ambiguity that the def2-TZVPPD basis set provides more quantitative agreement between experiment and theory for Rb^+(His), whereas the distinction is less clear for Cs^+(His). Previous results for other Rb^+(amino acid) and Cs^+(amino acid) complexes have found def2-TZVPPD BDEs superior to those obtained using HW* when compared to experiment.[11,12]

Comparison to Literature Bond Energies. Bojesen et al.[21] found that the sodium cation binding affinity for His lies between Asn and Arg in their relative measurements of the sodium cation affinities of the amino acids. Kish et al.[26] make a similar finding, locating its affinity as 57.4 ± 4 kJ/mol above that of Gly. Previously, we have measured D_0(Na^+−Gly) as 164.0 ± 6.0 kJ/mol[2,6] compared to the present value of D_0(Na^+−His) = 222.5 ± 11.0 kJ/mol. This yields a difference in sodium cation affinities of 58.5 ± 11.0 kJ/mol at 0 K (where the relative uncertainty in our measurements is smaller than the combined absolute uncertainties because various systematic errors in the measurements cancel). This value translates to a difference at 298 K of 58.0 ± 11.0 kJ/mol, in good agreement with the value of Kish et al. The absolute value reported by Kish et al. for D_{298}(Na^+−His) is 219 ± 8 kJ/mol, which translates to D_0(Na^+−His) = 217 ± 8 kJ/mol, but this scale is anchored to a value for Ala of 167 ± 8 kJ/mol. If anchored to our value of D_0(Na^+−Gly), their absolute value for D_0(Na^+−His) becomes 222 ± 8 kJ/mol. Either the original or reanchored value is in excellent agreement with the value obtained here.

Side-Chain Substituent Effect. The interactions of metal cations with amino acids are largely electrostatic, involving ion induced-dipole, ion-dipole, and ion-quadrupole forces, and lead to solvation of the charge by coordination of the amino acid functional groups. The BDEs required to remove the alkali metal cation from M^+(His), where M^+ = Na^+, K^+, Rb^+, and Cs^+ (Table 4), decrease from Na^+ to Cs^+. This is because the size of the metal cation increases (radii of 0.98, 1.33, 1.49, and 1.69 Å, respectively),[101] leading to longer metal−ligand distances that decrease the strength of the electrostatic interactions. The M^+(His) BDEs decline approximately 59 kJ/mol (~36%) as the metal changes from Na^+ to K^+, by another 26 kJ/mol (~19%) from K^+ to Rb^+, and then by 19 kJ/mol (~16%) in going to Cs^+. The relative BDE decreases are at the upper end of those measured in our laboratory for M^+(Gly), M^+(Pro), M^+(Ser), M^+(Thr), M^+(Met), and M^+(Cys): 23−32% for Na^+ to K^+, 10−20% for K^+ to Rb^+, and 6−17% for Rb^+ to Cs^+.[2,3,5,6,9−12] When the M^+(His) BDEs are compared to those of metal cationized aliphatic amino acids, such as M^+(Gly), as well as other bidentate amino acids such as M^+(Pro), they are generally larger because the side-chain imidazole group participates in the bonding. Compared to the M^+(Gly) systems, the binding energies of M^+(His) are increased by ~58 kJ/mol (~36%) for Na^+, ~43 kJ/mol (~35%) for K^+, ~28 kJ/mol (~26%) for Rb^+, and ~25 kJ/mol (~27%) for Cs^+. These changes are larger than those for the hydroxyl side chains of Ser and Thr, with increases of ~38 kJ/mol (~22%) for Na^+, ~26 kJ/mol (~21%) for K^+, ~10 kJ (~9%) for Rb^+, and ~11 kJ (~11%) for Cs^+. Note that for Ser, Thr, and His, the percent enhancements for Na^+ and K^+ are larger than those for Rb^+ and Cs^+, an observation discussed further below.

The influence of the side chain is also elucidated by examination of how the BDEs depend on the polarizability of the amino acid. As originally outlined by Rodgers and Armentrout,[1,4] there is an approximate linear dependence of the Na^+ and K^+ BDEs with the polarizability of the amino acids: Gly (6.6 Å^3), Pro (10.3 Å^3), Met (14.6 Å^3), Phe (18.1 Å^3), Tyr (18.8 Å^3), and Trp (22.0 Å^3). (All isotropic molecular polarizabilities used here were calculated at the PBE0/6-

311+G(2d,2p) level of theory using the B3LYP/6-311G(d,p) optimized geometries of the neutral amino acid in the metal cationized complexes. This level of theory has been shown to provide polarizabilities that are in good agreement with measured values.[102]) This trend quantifies the importance of ion-induced dipole interactions on the BDEs. Here, we reproduce this correlation in Figure 4 excluding Pro as it is

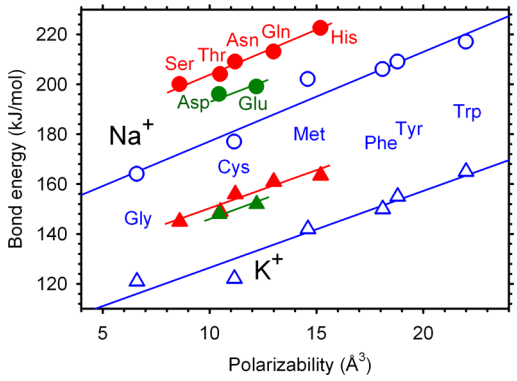

Figure 4. Experimental 0 K bond dissociation energies (in kJ/mol) for Na^+(amino acid) (circles) and K^+(amino acid) (triangles) versus the calculated polarizability (in Å^3) of the amino acid. The blue lines show linear regression analyses of the data, whereas red and green lines retain the same slopes (i.e., are parallel to the regressions).

zwitterionic and actually falls off the correlation line for both Na^+ and K^+. Subsequently, it has also been shown that Na^+ and K^+ BDEs to Ser (8.6 Å^3), Thr (10.5 Å^3), Asp (10.4 Å^3), Asn (11.2 Å^3), Glu (12.2 Å^3), and Gln (13.0 Å^3) do not fall on the same correlation line, but rather on lines parallel with those for Gly, Pro, Met, Phe, Tyr, and Trp,[9] as also reproduced in Figure 4. We attributed these differences to the local dipole moment of the side-chain coordinating site. Met, Phe, Tyr, and Trp have small side-chain dipoles, whereas Ser, Thr, Asn, and Gln have larger side-chain dipoles, with values for Asp and Glu being intermediate. In accord with these observations, the contribution of the side-chain dipole of His is appreciable. Consequently, even though His has a polarizability (15.2 Å^3) comparable to Met (14.6 Å^3), it binds to the alkali cations much more tightly, nicely in line with the Ser, Thr, Asn, and Gln progression, Figure 4. Indeed, the BDEs of His exceed those of Trp, which has a much higher polarizability. These comparisons are consistent with dipole moments for molecules corresponding to the side chains, namely, acetamide (mimicking Asn and Gln) and imidazole (His) have dipole moments of 3.68 and 3.8 D, whereas that for acetic acid (Asp and Glu) is about half that at 1.70 D.[103] Interestingly, methanol (mimicking Ser and Thr) also has a dipole of 1.70 D, suggesting that the alignment of the dipole as well as its magnitude are influential in the side-chain enhancements observed here. The ability to align favorably is probably related to the length of the side chain, with the two atom lengths (from backbone C_α to coordinating atom) of Ser and Thr being more restrictive than the three atom (Asn, Asp, His) and four atom (Gln, Glu) lengths.

For the Rb^+ and Cs^+ systems, there is insufficient data to analyze the trends in the same fashion; however, some insight into these trends can be obtained by viewing the periodic trends in the BDEs relative to the size of the metal cation, as previously assessed for Gly, Pro, Ser, Thr, and Cys.[11,12] As noted above, the BDEs decrease systematically from Li^+ to Cs^+ because the electrostatic interactions decrease with the increasing bond distances necessitated by the increasing size of the metal cation (radii of 0.70, 0.98, 1.33, 1.49, and 1.69 Å, respectively[101]). This is shown in Figure 5, where the lines are

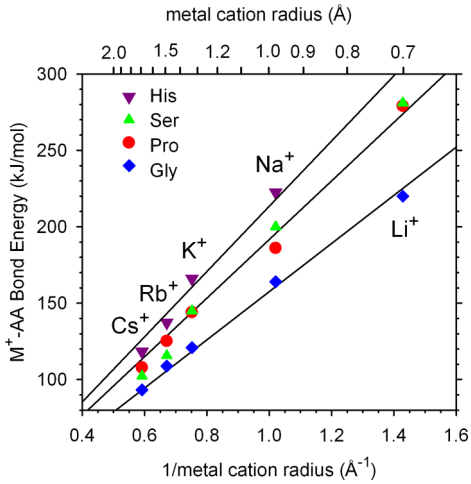

Figure 5. Experimental 0 K bond dissociation energies (in kJ/mol) for M^+(Gly) (blue diamonds), M^+(Pro) (red circles), M^+(Ser) (light green triangles), and M^+(His) (purple inverted triangles) for $M^+ = Li^+$, Na^+, K^+, Rb^+, and Cs^+ versus the inverse metal cation radius (in Å^{-1}). The lines are linear regression fits to the M^+(Gly), M^+(Pro), and M^+(His) data constrained to pass through the origin.

correlations of the M^+(Gly), M^+(Pro), and M^+(His) data constrained to pass through the origin. It can be seen that the data for all five alkali metal cations correlates reasonably well with the inverse of the metal cation radius for both M^+(Gly) and M^+(Pro). For M^+(Ser), it can be seen that the data for the smaller cations has a correlation similar to that for M^+(Pro), whereas the BDEs for Rb^+(Ser) and Cs^+(Ser) fall below the correlation, suggesting that the side chain does not enhance the binding as much as for the larger metal cations (as noted quantitatively above). Similar observations have also been made for M^+(Thr) and M^+(Cys).[12] M^+(His) shows a similar pattern in that the relative enhancement for the smaller cations is 50% larger than for the larger cations (noted above). In all these cases, this variation is probably associated with the change in geometry from tridentate to bidentate as the metal cation gets larger.

This hypothesis can be scrutinized further by examining the metal ligand bond lengths calculated for these complexes as a function of the metal cation identity. All calculated M^+–His bond lengths are found to increase approximately linearly with the metal cation radius with an intercept (cation radius = 0 Å) of 1.07–1.34 Å for all three conformers considered here. For the metal–carbonyl bond lengths associated with the [CO,N_α,N_π], [CO,N_π], and [COOH] geometries, the correlations increase linearly with slopes of 0.97–1.01, i.e., close to a slope of unity that would exactly match the increase with cation radius. In contrast, the metal cation–ligand distances for the other binding sites increase more rapidly with the cation radius: slopes of 1.12 for the M^+–N_α and M^+–N_π bonds in tridentate [CO,N_α,N_π], and 1.26 for M^+–N_π in bidentate [CO,N_π] and M^+–OH in bidentate [COOH]. As demonstrated previously for Na^+ and K^+,[2,3] the carbonyl is the most strongly binding site in amino acids. Therefore, the M^+–OC bond lengths are the shortest of all interactions and most

dx.doi.org/10.1021/jp310179c | J. Phys. Chem. A 2012, 116, 11823–11832

closely follow the metal cation radius. The weaker amino, imidazole, and hydroxyl binding sites[2,3] increase more rapidly because the multidentate nature of the binding limits the ability of the ions to bind equivalently at all sites. This leads to the complexes to the smaller cations having a clear tridentate [CO,$N_{\sigma}N_{\pi}$] GS conformer, whereas the energies of the bidentate [CO,N_{π}] and [COOH] conformers are lower than these for the larger metal cations.

CONCLUSIONS

The kinetic energy dependences of the collision-induced dissociation (CID) of M^+(His), where M^+ = Na^+, K^+, Rb^+, and Cs^+, are examined in guided ion beam tandem mass spectrometers. The only dissociation channel observed in all cases is the loss of the intact amino acid from the complex. The apparent threshold for removing His follows the order of Na^+(His) > K^+(His) > Rb^+(His) > Cs^+(His), as expected for the variations in charge density on the metal ion. BDEs at 0 K for losing His from the complexes, Table 2, are obtained by detailed modeling of the experimental cross sections.

Three different levels of quantum chemical calculations using two different basis sets including zero point energy corrections and counterpoise corrections for basis set superposition errors were performed for all M^+(His) complexes. The calculated BDEs for losing His from the M^+(His) complexes agree well with our experimental values, Table 4. As found previously, the HW* basis set for Rb and Cs underestimates the BDEs by about 8 kJ/mol, whereas the def2-TZVPPD basis sets yield theoretical values that are generally in good agreement with experiment, as previously found for other complexes of Rb^+ and Cs^+.[11,12,80]

The experimental 0 K BDEs of M^+(His) are larger than those of other M^+(amino acid) complexes available. This is attributed to contributions from the local dipole moment of the imidazole side chain functionality. Such contributions are found to be particularly important for the smaller cations, Na^+ and K^+, and weaker for Rb^+ and Cs^+. This is probably associated with the change in geometry from tridentate to bidentate as the metal cation gets larger.

AUTHOR INFORMATION

Present Address

[§]Abdullah Gul University, Kayseri, Turkey.

Notes

The authors declare no competing financial interest.

ACKNOWLEDGMENTS

This work is supported by the National Science Foundation, CHE-1049580 (P.B.A.) and CHE-0911191 (M.T.R.). A grant of computer time from the Center for High Performance Computing at the University of Utah is gratefully acknowledged.

REFERENCES

(1) Rodgers, M. T.; Armentrout, P. B. *Acc. Chem. Res.* **2004**, *37*, 989–998.
(2) Moision, R. M.; Armentrout, P. B. *J. Phys. Chem. A* **2002**, *106*, 10350–10362.
(3) Moision, R. M.; Armentrout, P. B. *Phys. Chem. Chem. Phys.* **2004**, *6*, 2588–2599.
(4) Ruan, C.; Rodgers, M. T. *J. Am. Chem. Soc.* **2004**, *126*, 14600–14610.
(5) Moision, R. M.; Armentrout, P. B. *J. Phys. Chem. A* **2006**, *110*, 3933–3946.
(6) Ye, S. J.; Clark, A. A.; Armentrout, P. B. *J. Phys. Chem. B* **2008**, *112*, 10291–10302.
(7) Heaton, A. L.; Moision, R. M.; Armentrout, P. B. *J. Phys. Chem. A* **2008**, *112*, 3319–3327.
(8) Heaton, A. L.; Armentrout, P. B. *J. Phys. Chem. B* **2008**, *112*, 12056–12065.
(9) Armentrout, P. B.; Gabriel, A.; Moision, R. M. *Int. J. Mass Spectrom.* **2009**, *283*, 56–68.
(10) Armentrout, P. B.; Armentrout, E. I.; Clark, A. A.; Cooper, T. E.; Stennett, E. M. S.; Carl, D. R. *J. Phys. Chem. B* **2010**, *114*, 3927–3937.
(11) Bowman, V. N.; Heaton, A. L.; Armentrout, P. B. *J. Phys. Chem. B* **2010**, *114*, 4107–4114.
(12) Armentrout, P. B.; Chen, Y.; Rodgers, M. T. *J. Phys. Chem. A* **2012**, *116*, 3989–3999.
(13) Dodson, G.; Wlodawer, A. *Trends Biochem. Sci.* **1998**, *23*, 347–352.
(14) Sundberg, R. J.; Martin, R. B. *Chem. Rev.* **1974**, *74*, 471–517.
(15) Harding, M. M.; Long, H. A. *J. Chem. Soc. A* **1968**, 2554–2559.
(16) Candlin, R.; Harding, M. M. *J. Chem. Soc. A* **1970**, 384–393.
(17) Fraser, K. A.; Harding, M. M. *J. Chem. Soc. A* **1967**, 415–420.
(18) Kretsinger, R. H.; Cotton, F. A.; Bryan, R. F. *Acta Crystallogr.* **1963**, *16*, 651–657.
(19) Evertsson, B. *Acta Crystallogr. B* **1969**, *25*, 30–41.
(20) Adams, M. J.; Hodgkin, D. C.; Raeburn, U. A. *J. Chem. Soc. A* **1970**, 2632–2635.
(21) Bojesen, G.; Breindahl, T.; Andersen, U. N. *Org. Mass Spectrom.* **1993**, *28*, 1448–1452.
(22) Andersen, U. N.; Bojesen, G. *J. Chem. Soc., Perkins Trans. 2* **1997**, 323–326.
(23) Hoyau, S.; Norrman, K.; McMahon, T. B.; Ohanessian, G. *J. Am. Chem. Soc.* **1999**, *121*, 8864–8875.
(24) Cerda, B. A.; Wesdemiotis, C. *Analyst* **2000**, *125*, 657–660.
(25) Ryzhov, V.; Dunbar, R. C.; Cerda, B. A.; Wesdemiotis, C. *J. Am. Soc. Mass Spectrom.* **2000**, *11*, 1037–1046.
(26) Kish, M. M.; Ohanessian, G.; Wesdemiotis, C. *Int. J. Mass Spectrom.* **2003**, *227*, 509–524.
(27) Feng, W. Y.; Gronert, S.; Lebrilla, C. B. *J. Phys. Chem. A* **2003**, *107*, 405–410.
(28) Kapota, C.; Lemaire, J.; Maitre, P.; Ohanessian, G. *J. Am. Chem. Soc.* **2004**, *126*, 1836–1842.
(29) Cooks, R. G.; Wong, P. H. *Acc. Chem. Res.* **1998**, *31*, 379–386.
(30) Cooks, R. G.; Koskinen, J. T.; Thomas, P. D. *J. Mass Spectrom.* **1999**, *34*, 85–92.
(31) Lau, J. K.-C.; Wong, C. H. S.; Ng, P. S.; Siu, F. M.; Ma, N. L.; Tsang, C. W. *Chem.—Eur. J.* **2003**, *9*, 3383–3396.
(32) Cerda, B. A.; Wesdemiotis, C. *J. Am. Chem. Soc.* **1995**, *117*, 9734–9739.
(33) Lee, V. W.-M.; Li, H.; Lau, T.-C.; Guevremont, R.; Siu, K. W. M. *J. Am. Soc. Mass Spectrom.* **1998**, *9*, 760–766.
(34) Jensen, F. *J. Am. Chem. Soc.* **1992**, *114*, 9533–9537.
(35) Hoyau, S.; Ohanessian, G. *Chem.—Eur. J.* **1998**, *4*, 1561–1569.
(36) Marino, T.; Russo, N.; Toscano, M. *Inorg. Chem.* **2001**, *40*, 6439–6443.
(37) Marino, T.; Russo, N.; Toscano, M. *J. Phys. Chem. B* **2003**, *107*, 2588–2594.
(38) Marino, T.; Russo, N.; Toscano, M. *J. Inorg. Biochem.* **2000**, *79*, 179–185.
(39) Polfer, N. C.; Oomens, J.; Dunbar, R. C. *Phys. Chem. Chem. Phys.* **2006**, *8*, 2744–2751.
(40) Forbes, M. W.; Bush, M. F.; Polfer, N. C.; Oomens, J.; Dunbar, R. C.; Williams, E. R.; Jockusch, R. A. *J. Phys. Chem. A* **2007**, *111*, 11759–11770.
(41) Armentrout, P. B.; Rodgers, M. T.; Oomens, J.; Steill, J. D. *J. Phys. Chem. A* **2008**, *112*, 2248–2257.
(42) Rodgers, M. T.; Armentrout, P. B.; Oomens, J.; Steill, J. D. *J. Phys. Chem. A* **2008**, *112*, 2258–2267.

(43) O'Brien, J. T.; Prell, J. S.; Steill, J. D.; Oomens, J.; Williams, E. R. *J. phys. Chem. A* **2008**, *112*, 10823−10830.
(44) Klassen, J. S.; Anderson, S. G.; Blades, A. T.; Kebarle, P. *J. Phys. Chem.* **1996**, *100*, 14218−14227.
(45) Heaton, A. L.; Bowman, V. N.; Oomens, J.; Steill, J. D.; Armentrout, P. B. *J. Phys. Chem. A* **2009**, *113*, 5519−5530.
(46) Carl, D. R.; Cooper, T. E.; Oomens, J.; Steill, J. D.; Armentrout, P. B. *Phys. Chem. Chem. Phys.* **2010**, *12*, 3384−3398.
(47) Citir, M.; Stennett, E. M. S.; Oomens, J.; Steill, J. D.; Rodgers, M. T.; Armentrout, P. B. *Int. J. Mass Spectrom.* **2010**, *297*, 9−17.
(48) Citir, M.; Hinton, C. S.; Oomens, J.; Steill, J. D.; Armentrout, P. B. *J. Phys. Chem. A* **2012**, *116*, 1532−1541.
(49) Hay, P. J.; Wadt, W. R. *J. Chem. Phys.* **1985**, *82*, 299−310.
(50) Glendening, E. D.; Feller, D.; Thompson, M. A. *J. Am. Chem. Soc.* **1994**, *116*, 10657−10669.
(51) Ervin, K. M.; Armentrout, P. B. *J. Chem. Phys.* **1985**, *83*, 166−189.
(52) Muntean, F.; Armentrout, P. B. *J. Chem. Phys.* **2001**, *115*, 1213−1228.
(53) Rodgers, M. T. *J. Phys. Chem. A* **2001**, *105*, 2374−2383.
(54) Fenn, J. B.; Mann, M.; Meng, C. K.; Wong, S. F.; Whitehouse, C. M. *Mass Spectrom. Rev.* **1990**, *9*, 37−70.
(55) Moision, R. M.; Armentrout, P. B. *J. Am. Soc. Mass Spectrom.* **2007**, *18*, 1124−1134.
(56) Kim, T.; Tolmachev, A. V.; Harkewicz, R.; Prior, D. C.; Anderson, G.; Udseth, H. R.; Smith, R. D. *Anal. Chem.* **2000**, *72*, 2247−2255.
(57) Carl, D. R.; Moision, R. M.; Armentrout, P. B. *Int. J. Mass Spectrom.* **2007**, *265*, 308−325.
(58) Ye, S. J.; Armentrout, P. B. *J. Phys. Chem. A* **2008**, *112*, 3587−3596.
(59) Chen, Y.; Rodgers, M. T. *J. Am. Chem. Soc.* **2012**, *134*, 2313−2324.
(60) Chen, Y.; Rodgers, M. T. *J. Am. Chem. Soc.* **2012**, *134*, 5863.
(61) Gerlich, D. *Adv. Chem. Phys.* **1992**, *82*, 1−176.
(62) Hales, D. A.; Lian, L.; Armentrout, P. B. *Int. J. Mass Spectrom. Ion Processes* **1990**, *102*, 269−301.
(63) Daly, N. R. *Rev. Sci. Instrum.* **1960**, *31*, 264−267.
(64) Beyer, T. S.; Swinehart, D. F. *Commun. ACM* **1973**, *16*, 379.
(65) Stein, S. E.; Rabinovich, B. S. *J. Chem. Phys.* **1973**, *58*, 2438−2445.
(66) Stein, S. E.; Rabinovich, B. S. *Chem. Phys. Lett.* **1977**, *49*, 183−188.
(67) Gilbert, R. G.; Smith, S. C. *Theory of Unimolecular and Recombination Reactions*; Blackwell Scientific: London, 1990.
(68) Truhlar, D. G.; Garrett, B. C.; Klippenstein, S. J. *J. Phys. Chem.* **1996**, *100*, 12771−12800.
(69) Holbrook, K. A.; Pilling, M. J.; Robertson, S. H. *Unimolecular Reactions*, 2nd ed.; Wiley: New York, 1996.
(70) Rodgers, M. T.; Ervin, K. M.; Armentrout, P. B. *J. Chem. Phys.* **1997**, *106*, 4499−4508.
(71) Rodgers, M. T.; Armentrout, P. B. *J. Chem. Phys.* **1998**, *109*, 1787−1800.
(72) Armentrout, P. B.; Ervin, K. M.; Rodgers, M. T. *J. Phys. Chem. A* **2008**, *112*, 10071−10085.
(73) Meyer, F.; Khan, F. A.; Armentrout, P. B. *J. Am. Chem. Soc.* **1995**, *117*, 9740−9748.
(74) Rodgers, M. T.; Armentrout, P. B. *J. Phys. Chem. A* **1997**, *101*, 1238−1249.
(75) Koizumi, H.; Armentrout, P. B. *J. Am. Soc. Mass Spectrom.* **2001**, *12*, 480−489.
(76) Ye, S. J.; Moision, R. M.; Armentrout, P. B. *Int. J. Mass Spectrom.* **2006**, *253*, 288−304.
(77) More, M. B.; Ray, D.; Armentrout, P. B. *J. Phys. Chem. A* **1997**, *101*, 831−839.
(78) More, M. B.; Ray, D.; Armentrout, P. B. *J. Phys. Chem. A* **1997**, *101*, 4254−4262.
(79) More, M. B.; Ray, D.; Armentrout, P. B. *J. Phys. Chem. A* **1997**, *101*, 7007−7017.
(80) Armentrout, P. B.; Austin, C. A.; Rodgers, M. T. *Int. J. Mass Spectrom.* **2013**, DOI: 10.1016/j.ijms.2012.06.018.
(81) Waage, E. V.; Rabinovitch, B. S. *Chem. Rev.* **1970**, *70*, 377−387.
(82) Armentrout, P. B.; Simons, J. *J. Am. Chem. Soc.* **1992**, *114*, 8627−8633.
(83) Frisch, M. J.; Trucks, G. W.; Schlegel, H. B.; Scuseria, G. E.; Robb, M. A.; Cheeseman, J. R.; Scalmani, G.; Barone, V.; Mennucci, B.; Petersson, G. A.; et al. *Gaussian 09*; Gaussian Inc.: Pittsburgh, PA, 2009.
(84) Foresman, J. B.; Frisch, A. E. *Exploring Chemistry with Electronic Structure Methods*, 2nd ed.; Gaussian, Inc.: Pittsburgh, PA, 1996.
(85) Weigend, F.; Ahlrichs, R. *Phys. Chem. Chem. Phys.* **2005**, *7*, 3297.
(86) Leininger, T.; Nicklass, A.; Kuechle, W.; Stoll, H.; Dolg, M.; Bergner, A. *Chem. Phys. Lett.* **1996**, *255*, 274−280.
(87) Boys, S. F.; Bernardi, R. *Mol. Phys.* **1970**, *19*, 553−566.
(88) van Duijneveldt, F. B.; van Duijneveldt de Rijdt, J. G. C. M.; van Lenthe, J. H. *Chem. Rev.* **1994**, *94*, 1873−1885.
(89) Ye, S. J.; Moision, R. M.; Armentrout, P. B. *Int. J. Mass Spectrom.* **2005**, *240*, 233−248.
(90) Armentrout, P. B.; Rodgers, M. T. *J. Phys. Chem. A* **2000**, *104*, 2238−2247.
(91) Huang, Z.; Yu, W.; Lin, Z. *J. Mol. Struct.: THEOCHEM* **2006**, *801*, 7−20.
(92) Huang, Z.; Lin, Z.; Song, C. *J. Phys. Chem. A* **2007**, *111*, 4340−4352.
(93) IUPAC. *Compendium of Chemical Terminology*, 2nd ed. (the "Gold Book"); Blackwell Scientific Publications: Oxford, U.K., 1997. Compiled by A. D. McNaught and A. Wilkinson. XML on-line corrected version: http://goldbook.iupac.org (2006-) created by M. Nic, J. Jirat, and B. Kosata. Updates compiled by A. Jenkins. ISBN 0-9678550-9-8. DOI10.1351/goldbook.
(94) Shoeib, T.; Siu, K. W. M.; Hopkinson, A. C. *J. Phys. Chem. A* **2002**, *106*, 6121−6128.
(95) Dunbar, R. C.; Hopkinson, A. C.; Oomens, J.; Siu, C.-K.; Siu, K. W. M.; Steill, J. D.; Verkerk, U. H.; Zhao, J. *J. Phys. Chem. B* **2009**, *113*, 10403−10408.
(96) Rodriguez-Santiago, L.; Sodupe, M.; Tortajada, J. *J. Phys. Chem. A* **2001**, *105*, 5340−5347.
(97) Bertran, J.; Rodriguez-Santiago, L.; Sodupe, M. *J. Phys. Chem. B* **1999**, *103*, 2310−2317.
(98) Rodgers, M. T.; Armentrout, P. B. *Mass Spectrom. Rev.* **2000**, *19*, 215−247.
(99) Rodgers, M. T.; Armentrout, P. B. *Int. J. Mass Spectrom.* **1999**, *185/186/187*, 359−380.
(100) Lifshitz, C. *Adv. Mass Spectrom.* **1989**, *11*, 713−729.
(101) Wilson, R. G.; Brewer, G. R. *Ion Beams with Applications to Ion Implantation*; Wiley: New York, 1973.
(102) Smith, S. M.; Markevitch, A. N.; Romanor, D. A.; Li, X.; Levis, R. J.; Schlegel, H. B. *J. Phys. Chem. A* **2000**, *108*, 11063−11072.
(103) *Handbook of Chemistry and Physics*; CRC Press: Boca Raton, FL, 2002.